PAPER

Novel 3D lightweight carbon foam as an effective adsorbent for arsenic(v) removal from contaminated water

Pinki Rani Agrawal,[ac] Rajeev Kumar,[a] Himani Uppal,[bc] Nahar Singh,[b] Saroj Kumari[a] and Sanjay R. Dhakate*[a]

In the present work, an efficient system for removal of pentavalent arsenic (As(v)) from water has been developed using a novel three-dimensional (3D) lightweight carbon foam. The carbon foam was synthesized from phenolic resin by a sacrificial template technique followed by stabilisation and carbonisation. The carbon foam was characterized by X-ray diffraction (XRD) for phase identification and energy dispersive spectroscopy (EDS) for compositional analysis. This same carbon foam has been utilized for the removal of As(v), and remaining concentrations were determined using an atomic absorption spectrophotometer-hydride generator (AAS-HG) at varying adsorption parameters, *viz.* time, pH and adsorbate dose. The adsorption data is best fitted to a Langmuir isotherm and suggests monolayer adsorption over a homogenous surface. The adsorption capacity of carbon foam is 38.4 µg g^{-1} and the % of arsenic removal is 99.1%, which is very high as compared to other low density carbon materials. The carbon foams efficiently adsorbed As(v) and purify water below the prescribed limits of the world health organization (WHO) and the United States-environmental protection agency (US-EPA).

1. Introduction

The natural as well as anthropogenic contamination of toxic metals (mercury, cadmium, lead, arsenic, chromium) in the environment as per the U.S. Environmental Protection Agency (US-EPA) are of major concern because of their toxicity, bio-accumulating tendency, and threat to human life and the environment.[1–4] Arsenic is one of the highly poisonous threats to the health of humans and ecological balance.[5] Widespread arsenic contamination in groundwater has led to a massive epidemic in Asia and America, especially in India, Bangladesh, Vietnam, Cambodia, Thailand, southwest USA, Canada, Chile *etc.* Thus, the remediation of arsenic pollution has attracted worldwide attention.[6,7]

Arsenic concentration in various water bodies is increasing day by day due to several reasons like use of arsenical pesticides, mineral dissolution, mine drainage, disposal of fly ash, and geothermal discharge. According to the European Commission, WHO and US-EPA, the acceptable limit of arsenic in drinking water is 10 µg L^{-1}.[8] The long-term even low concentration of As(v) in drinking water disturbs the normal functioning of nervous and cardiovascular system and also increases the risk of cancer of skin, kidney, liver, and prostate.[9,10]

Several technologies reported in the literature for As(v) removal are precipitation, nanofiltration, reverse osmosis, electrodialysis, adsorption, ion exchange, solvent extraction, and bioremediation.[11–16] Most of these techniques are well-established and have their merits and inherent limitations such as the generation of toxic waste, low as removal efficiencies, and high cost.[17] Among these techniques, adsorption has been recognized to be an efficient technique for As(v) removal. Besides these several materials like lanthanum, iron compounds, mineral oxides, and biological materials[17,18] have been studied for As removal. The use of polymeric resins, activated carbon,[19] activated alumina, iron-coated sand,[20] hydrous ferric oxide,[21] natural ores and metal modified adsorbents have generated much interest for better performance.[22,23] Carbon materials like activated carbon, carbon fibers, carbon nanotubes (CNTs) and graphene have been studied for the removal of arsenic from ground water. Activated carbon and iron doped activated carbon have been developed for removing the arsenic from contaminated water due to selective affinity.[24,25] Graphene and carbon nanotubes (CNT) also act as good adsorbent for arsenic because it possesses fibrous shape with high aspect ratio, large surface area and well developed mesopores.[26,27] Liu *et al.* demonstrated TiO_2 coated carbon nanotube for removal of arsenic from contaminated water.[28] Vadahanambi *et al.* and Mitra *et al.* has also developed multiwalled carbon nanotube

aPhysics & Engineering of Carbon, Division of Material Physics and Engineering, CSIR-National Physical Laboratory, Dr. K.S. Krishnan Marg, New Delhi-110012, India. E-mail: dhakate@nplindia.org; Tel: +91-11-45609388

bAnalytical Chemistry Division, CSIR-National Physical Laboratory, Dr. K.S. Krishnan Marg, New Delhi-110012, India

cAcademy of Scientific and Innovative Research (AcSIR), India

(MWCNT) coated with Fe_3O_4 for removing even trace amount of arsenic to meet drinking water standards.[29,30]

Porous materials are good candidates for adsorption of heavy metals because of facile diffusion of reactants and products through the pores, regular and tunable pore size with uniform pore structure, and good physiochemical stability as well as their large surface area and pore volume.[31–33] It is known that porous carbon materials, which are thermally stable, chemically inert and low cost, show better adsorption property for heavy metals. Furthermore, Burke et al.[34] and Lee et al.[35] reported that mesoporous carbon foam have been used for the removal of copper and lead. Though significance progress has been made for the removal of heavy metals from water. However, nobody has reported yet the uptake proper mechanism and pathways for the removal of arsenic from water using carbon foam.

In view of above, we have fabricated 3D lightweight porous carbon foam of large and uniform pore size for the removal of As(v). The proposed fabricated carbon foam have interconnected pores having large surface area, large pore volume and provides several advantages over other types of mesoporous as well as carbon nanomaterials. The carbon foam was fabricated by dipping polyurethane foam template in phenol formaldehyde solution followed by oxidation at 300 °C for 15 h in air atmosphere. Further carbonization was done at 1000 °C in inert atmosphere.

2. Experimental procedure

2.1. Chemicals and materials

For the fabrication of carbon foam polyurethane foam (PU) as template was procured from S. G. & Company, New Delhi-India. The chemicals for the fabrications, As(v) removal studies and potentiometric titration like phenol formaldehyde, acetone, sodium borohydride, hydrochloric acid, sodium hydroxide, potassium hydroxide, nitric acid, sodium salt of ethylene diamine tetra acetic acid, potassium nitrate etc. were procured from E. Merck India. All the chemicals used were of analytical grade. Double distilled water was used for the fabrication related work, while de-ionized water of 18.2 mega Ω resistivity (Millipore, Milli-Q element-USA) was used for absorption studies. The As(v) removal studies and calibration of AAS-HG was done using Merck Germany make traceable certified reference standard after appropriate dilutions. All the glassware used for fabrication and experimental studies were procured from Borosil India limited. The pH during experiments was adjusted using Orion make 3-star benchtop pH meter.

2.2. Fabrication of carbon foam

Carbon foam has been fabricated by the sacrificial template route by impregnating phenolic resin in the commercially available PU foams.[36–39] The PU foams slabs (density, 0.030 g cm^{-3}, cell size 0.45 mm; cell number per unit length, 50 pores per inch) were used as a template. The templates were dipped into 35% of phenolic resin in organic solvent like acetone. Initially porous PU foam slabs (average dimensions: 30 mm × 20 mm × 10 mm) have been cleaned with distilled water and dried in air at 100 °C for 6 h. The dried foams were then dipped

repeatedly 2–3 times into phenolic resin solution. The impregnated foams were dried in an oven at 100 °C for 12 h in order to evaporate organic solvent. The dried foams were then oxidised at 300 °C (@10 °C h^{-1}) in air atmosphere for one hour. This heat treatment process at 300 °C has been carried out for stabilization of the interconnected resin network by introducing cross-links in the structure. Further the dried foams were carbonized at 1000 °C for 1 hour in inert atmosphere and resultant carbon foam having a bulk densities in the range of 0.25–0.35 g cm^{-3}. The dried foams were then used for As(v) removal process. A schematic diagram from fabrication to As(v) adsorption has been given in Fig. 1.

2.3. Characterization

The morphology of the carbon foams before and after removal of As(v) was observed by using scanning electron microscope [SEM (LEO 440)] from USA. FTIR studies were also carried out before and after removal of As(v) using thermo Nicolet model 380 procured from United Kingdom. The XPS spectra of carbon foam before and after removal of As(v) was obtained using a Multi Lab 2000 spectrometer (Thermo Electron Corporation, England) to investigate the elements composition and surface groups present on the surface of the carbon foam samples. Al Kα (1485.6 eV) was used as the X-ray source with a 14.9 keV anode voltage, a 4.6 A filament current and a 20 mA emission current. The XPS spectra were obtained with 50 eV pass energy and a 0.5 eV step size. Core level spectra were obtained at 20 eV pass energy with a 0.05 eV step size. The phase identification and crystallite size of pure foam and after As(v) adsorption were done using Rigaku powder X-ray diffractometer (model XRG 2kw) using Cu Kα radiation ($λ = 1.54059$ Å). The As(v) removal studies were carried out using Analytic Jena Germany make AAS-HG, model vario-6 at optimized conditions.

2.4. Point zero charge

Point of zero charge (pzc) is the pH of a material at which the surface of the material becomes neutrally charged. The pH_{pzc} of carbon foam has been confirmed using potentiometric titration.[40] To determine pH_{pzc}, carbon foam was dipped in 25 mL solution of 0.03 M KNO_3 solution and the solution was left overnight (24 h) under constant stirring for stabilizing the pH. Further 0.1 mL solution of 1 M KOH was added into the solution of KNO_3 and pH was recorded after each addition of 20 μL solution of 0.1 M HNO_3 using micropipette. Blank titration was also done in a similar way. The pH_{pzc} of the carbon foam was determined from the curve of pH against acid consumed as presented in Fig. 2(a).

2.5. Adsorption studies

For the As(v) adsorption study, the stock solution of As(v) of desired strength was prepared after appropriate dilution in de-ionized water. The pH of the solution was adjusted by adding solution of 0.001 M HCl and KOH. The carbon foam was dipped for 24 hours. The decanted solution was analyzed for left over concentration of As(v) using 3% sodium borohydride, 1.5% NaOH, and 2% HCl for arsenic hydride generation. Atomization
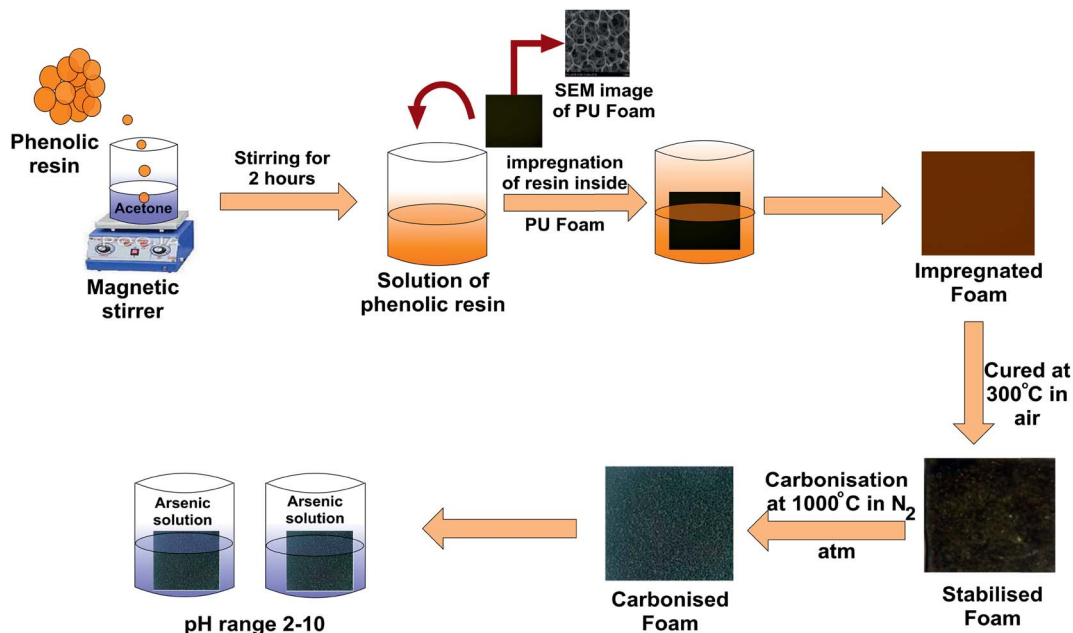
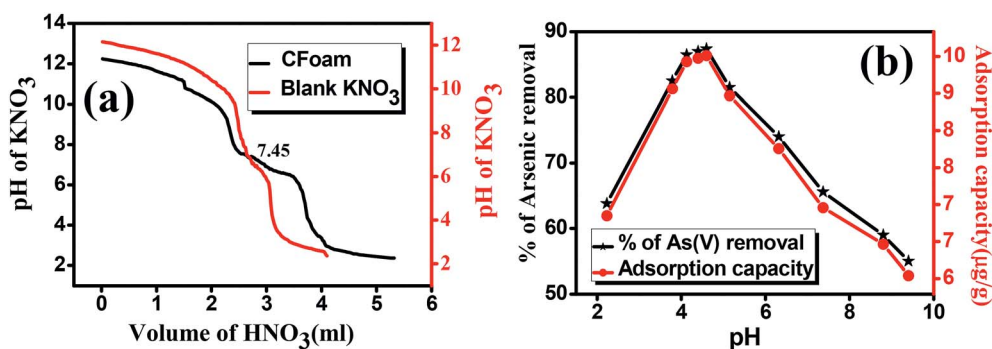**Fig. 1** Schematic diagram shows the fabrication process of carbon foam for the removal of As(v).

Fig. 2 (a) pH_{pzc} and (b) effect of pH on arsenic(v) adsorption capacity.

of As(v) was carried out at 900 °C using electro thermal heating in the presence of argon gas with 36 mL min^{-1} flow rate.[41] The adsorption capacity of carbon foam was calculated by using eqn (1) and (2)

$$\text{Adsorption capacity} = \frac{(C_i - C_f)}{w} \times V \qquad (1)$$

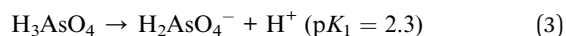$$\% \text{ of arsenic removal} = \frac{C_i - C_f}{C_i} \times 100 \qquad (2)$$

where C_i is initial concentration of arsenic(v) solution, C_f is the final concentration of As(v) remaining in the solution; V is the volume of solution, w is the weight of adsorbent (g).
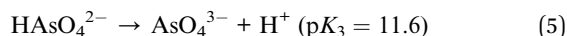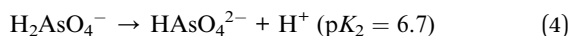
3. Results and discussion

3.1. Effect of pH

The pH of the aqueous solution is the most important factor for As(v) removal. The relationship between the pH and pH_{pzc} of

a solution has a significant effect on adsorption at the liquid–solid interface. As(v) species is present in water with three forms of which the acid base dissociation constant (pK_a) values are 2.2, 7.0 and 11.5 respectively.[42] $H_2AsO_4^-$ and $HAsO_4^{2-}$ are the main species which is found in natural water with pH range 5–8. For the optimization of pH several sets of solution were prepared by varying pH from 2 to 10 and in these solutions, carbon foams were dipped in these solutions and kept for 24 hours. The decanted solutions were analysed by AAS-HG for remaining concentration of As(v). The % removal of As(v) vs. pH has been presented in Fig. 2(b). From the figure it has been observed that maximum adsorption occurred between 4 to 5 pH, whereas on increasing pH above 5, there is a gradual decrease adsorption. The distribution profile was constructed as a function of solution pH based on the following three equilibrium and their respective stability constants.

$$H_3AsO_4 \rightarrow H_2AsO_4^- + H^+ \quad (pK_1 = 2.3) \qquad (3)$$

$$H_2AsO_4^- \rightarrow HAsO_4^{2-} + H^+ \ (pK_2 = 6.7) \tag{4}$$

$$HAsO_4^{2-} \rightarrow AsO_4^{3-} + H^+ \ (pK_3 = 11.6) \tag{5}$$

The pH_{pzc} of the carbon foam was observed to be 7.45, whereas maximum adsorption occurred between 4 and 5 pH ranges, which denote that the surface of the adsorbent is positively charged. The surface of the adsorbate is negatively charged ($H_2AsO_4^-$), while surface of adsorbent is positively charged and would be involved in protonation of –OH group. The positive surface of adsorbent (carbon foam) attracts the negative surface of adsorbate ($H_2AsO_4^-$) because of electrostatic interaction. The schematic diagram of possible chemical interaction is given in Fig. 3.

3.2. Structural and morphological analysis

The XPS is an excellent tool to identify the functional groups present on the surface of the material. The XPS spectra of carbon foam before and after As(v) adsorption were taken as given in Fig. 4(a–d). It consist of carbon C1s and oxygen O1s spectra, which is due to the electron transition from carbon–oxygen atoms of different atomic configuration and their shape depends upon atomic densities. The evaluation of bonding content consists of spectra background subtraction, followed by fitting of Gaussian–Lorentzian asymmetric functions to the measured spectra, selecting the relevant binding energy values from literature.[22] In both the cases, asymmetric peaks were observed centred at different binding energies with long tail extended to the higher energy region. In both the cases, (carbon foam before and after arsenic adsorption), the deconvolution of C1s spectra is split into four peaks as shown in Fig. 4(a) and (c). The first (C1s A) peak was observed at 284.5 eV of carbon (C–C) in graphitic type, second peak (C1s B) was found at 286.0 eV of carbon singly bound to oxygen (C–O) in phenols and ethers, third peak (C1s C) was found at 286.6 eV of carbon doubly

bound to oxygen (C=O) in ketones and quinones, and fourth peak (C1s D) at 289.2 of carbon bound to two oxygen (–COO) in carboxyl, carboxylic anhydrides and ester. Moreover, deconvolution of the O1s spectrum of both carbon foams split into two peaks (Fig. 4(b) and (d)), first oxygen doubly bound to carbon (O=C) at 533.2 eV in the form of quinones, ketones and aldehydes and second oxygen single bound to carbon (O–C) at 536.6 eV in the form of ethers and phenols. However, after adsorption of As(v), the carbon and oxygen peak area is gradually increase as show in Fig. 4(c) and (d). Fig. 4(e) shows the XPS spectra of As(v) in carbon foam after adsorption. The peaks at 43 and 45.26 eV are assigned As and As_2O_5 respectively.[43,44]

XRD spectra of carbon foam before and after As(v) adsorption are shown in Fig. 5(a) and (b) respectively. Two broad diffraction peaks at 24.9° and 43.1° are shown in Fig. 5(a) which correspond to the amorphous nature of carbon of (002) and (100) lattice plane, respectively, which is due to the turbostatic nature of phenolic resin at 1000 °C. This finding is due to the formation of glassy carbon structures from which is derived from thermosetting phenolic resin polymer. The peak at $2\theta = 24.9°$ corresponds to (002) plane of carbon materials. It is seen that the interlayer spacing (d_{002}) of pristine carbon foam is 0.3509 nm. However, after adsorption of As(v) onto the carbon foam, the peak at $2\theta = 24.9°$ is shifted to 25.1° as presented in Fig. 5(b). The shifting and increases in peak intensity confirms the presence of As(v) adsorption over the carbon foam.

The FTIR spectra of pristine carbon foam and carbon foam after As(v) adsorption recorded by varying wave number in the range of 4000–500 cm^{-1} are shown in Fig. 5(c) and (d). In both the samples, it can be seen that there are strong absorption peaks in the range of 3400–3700 cm^{-1}. These are due to –OH stretching vibrations; and indicate the presence of high content of hydroxyl groups present on the surface of carbon foam.

The absorption peaks at 3040 and 3042 cm^{-1} indicate the presence of sp^2 carbon (C=C). After As(v) adsorption by carbon foam (Fig. 5(d)), three new peaks are observed between the wave number of 800–1600 cm^{-1}, the peaks in this range are due to As(v) adsorption on the surface of carbon foam as confirmed by XRD. The peak at 1450 cm^{-1} indicates the symmetric and asymmetric stretching of COO$^-$ group and peak at 1060 cm^{-1} is due to C=O stretching of the COO$^-$ group and peak at 870 cm^{-1} is due to the –OH bonding.

SEM images of pristine carbon foam as well as after adsorption of As(v) are depicted in Fig. 6(a) and (b). As seen in Fig. 6(a), the carbon foam exhibits fairly surface and uniform pore size in the range 200–300 μm with a narrow ligaments. Also, virtually all cells are open and connected to several neighbouring cells. An XRD result shows that carbon foam having turbostatic structures (higher interlayer spacing) which correspond to the amorphous nature of carbon. However, when this carbon foam was used to remove As(v) from water there is some chemical reaction are occurred and form C–$H_2AsO_4^-$. Due to this chemical interaction and acidic nature of $H_2AsO_4^-$, carbon foam ligaments gets deformatted and wider as shown in Fig. 6(b), moreover, the surface of carbon foam is become coarser by deposition of As(v).
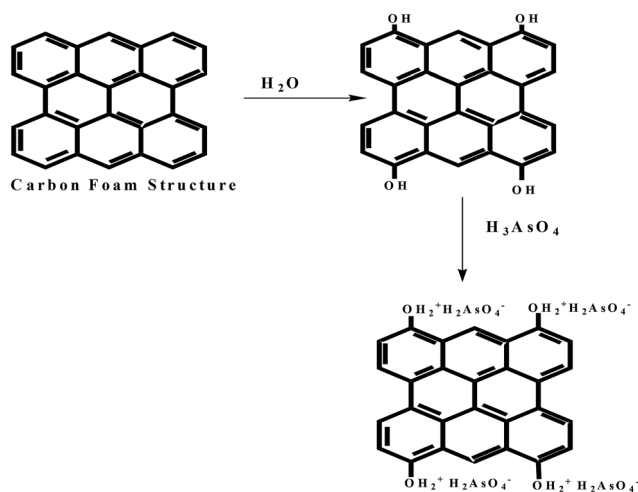

Fig. 3 Schematic diagram of chemical interaction between carbon foam and As(v).
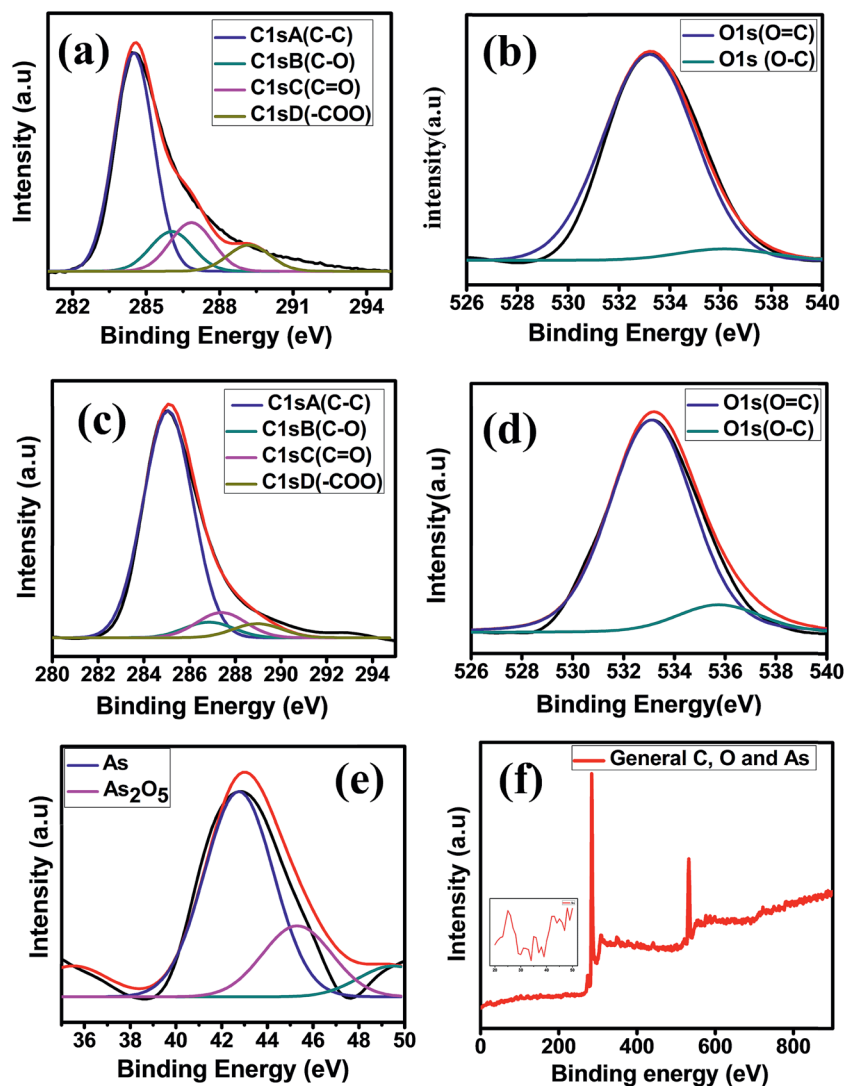
Fig. 4 XPS spectra of carbon foam before As(v) adsorption (a and b) and (c–f) after As(v) adsorption.

3.3. Kinetic study

Kinetic study is one of the most important characteristics that define the efficiency of adsorption. The experiment has been brought off with 1 mg L^{-1} concentration of As(v) at optimized parameters. Fig. 7 represents the adsorption efficiency of carbon foams with respect to time. It has been observed that maximum adsorption occurred in 6 hours. The proposed material effectively removed As(v) below prescribed limits of WHO. Fig. 7(a–d) represents percent removal, adsorption capacity, pseudo second order, and first order kinetics respectively. The pseudo second order kinetics has been given in eqn (6) and (7).

$$\frac{t}{q_t} = \frac{1}{k_2 q_e^2} + \frac{t}{q_e} \quad \text{(pseudo second order)} \quad (6)$$

In above equation, if time 't' is zero, then the initial sorption rate 'h' will be calculated using eqn (7).

$$h = k_2 q_e^2 \quad (7)$$

In above eqn (6) and (7), 'q_e' and 'q_t' (µg g^{-1}) are the adsorption capacity of carbon foam at equilibrium 'e' and at time 't' respectively, 'h' (µg g^{-1} min^{-1}) represents the initial adsorption rate and 'k_2' (g µg^{-1} min^{-1}) is the rate constant.

The pseudo first order kinetics (eqn (8)), represents the adsorption rates which depend either on the concentration of adsorbate or adsorbent.

$$\ln(q_e - q_t) = \ln q_e - k_1 t \quad \text{(pseudo first order)} \quad (8)$$

In eqn (8), 'q_e' and 'q_t' (µg g^{-1}) are the adsorption capacity of carbon foam at equilibrium 'e' and at time 't' respectively, 'k_1' is the rate constant (min^{-1}).

The adsorption kinetics experimental data was fitted to eqn (6) and (8) to study the adsorption behaviour of the carbon foam. This study suggests whether the material follow pseudo second or first order kinetics. Fig. 7(b) shows the adsorption capacity of carbon foam with respect to time. The adsorption capacity of the proposed carbon foam was found to be 10 µg
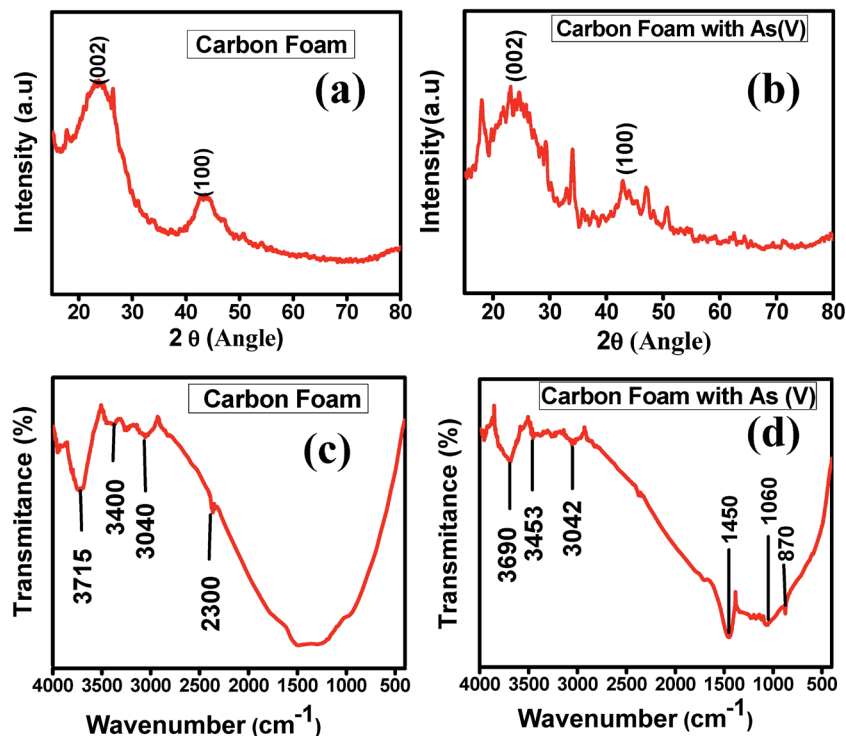
Fig. 5   (a) and (b) XRD spectra and (c) and (d) FTIR spectra of carbon foam before and after As(v) adsorption respectively.
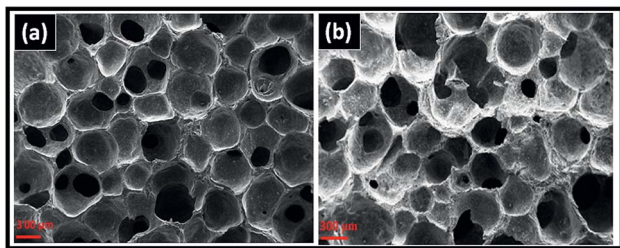

Fig. 6   SEM images of (a) pristine carbon foam, (b) after As(v) adsorption.

g^{-1}. Fig. 7(c) explains the pseudo second order kinetics equation with respect to adsorption capacity 't/q_t' vs. time 't'. The adsorption capacity 'q_e', adsorption rate 'h', rate constant 'k' and coefficient of determination 'R^2' was calculated by slope and intercept of Fig. 7(c). The value of 'h', 'k', and 'R^2' were found to be 8.0 μg g^{-1} min^{-1}, 0.0474 g μg^{-1} min^{-1} and 0.973 respectively. The adsorption capacity (q_e) was calculated from Fig. 7(c) and compare with the experimental data. It has been concluded that experimental adsorption capacity (10 μg g^{-1}) and theoretical adsorption capacity (13 μg g^{-1}) results are comparable. Fig. 7(d) represents the pseudo first order kinetic, and it has been observed that first order kinetics is not applicable for the proposed material. From the Fig. 7(d), the value of 'R^2' is found to 0.90, which is less than pseudo second order kinetics (0.97). We can be concluded that the adsorption kinetics follows second order kinetic and the adsorption rate of As(v) depends on the concentration of adsorbate and adsorbent.

3.4.   Adsorption isotherm

Adsorption isotherm describes the equilibrium relationship between solid and liquid interfaces and can be explained in the form of Langmuir, Freundlich, Temkin and Dubinin–Radushkevich (D–R) isotherms.[45] In the proposed study we have used only Langmuir, Freundlich isotherm to understand the behaviour of adsorbent and adsorbate. Langmuir isotherm suggests that adsorption of the metal ions occurs on a homogeneous surface by monolayer without any interaction between adsorbent and adsorbate. It also describes numbers of specific active sites which interacts with adsorbate molecules. Whereas, Freundlich adsorption isotherm suggests heterogeneous nature of adsorbent surface and multilayers adsorption of the adsorbate onto the surface of adsorbent.[46] The adsorption capacity of carbon foam for As(v) has been calculated using the equilibrium adsorption isotherm by varying the initial concentration of As(v) from 1 to 10 mg L^{-1} with fixed amount of adsorbent (approx. 1.8 g). All the experiments were carried out in 25 mL of As(v) solutions. Initially the adsorption capacity of carbon foam increases, which gradually decreases on increasing concentration of As(v) due to exhaust of active sites present over the surface of carbon foam. The maximum adsorption capacity of carbon foam was observed at 3 mg L^{-1} concentration within 6 hours and shown in Fig. 8(a).

The adsorption capacity of fixed amount of carbon foam vs. remaining concentration of As(v) data were fitted using Langmuir isotherm. The adsorption capacity of carbon foam was calculated using eqn (9) as given below;

$$\frac{C_f}{q_e} = \frac{1}{K_L q_m} + \frac{C_f}{q_m} \tag{9}$$
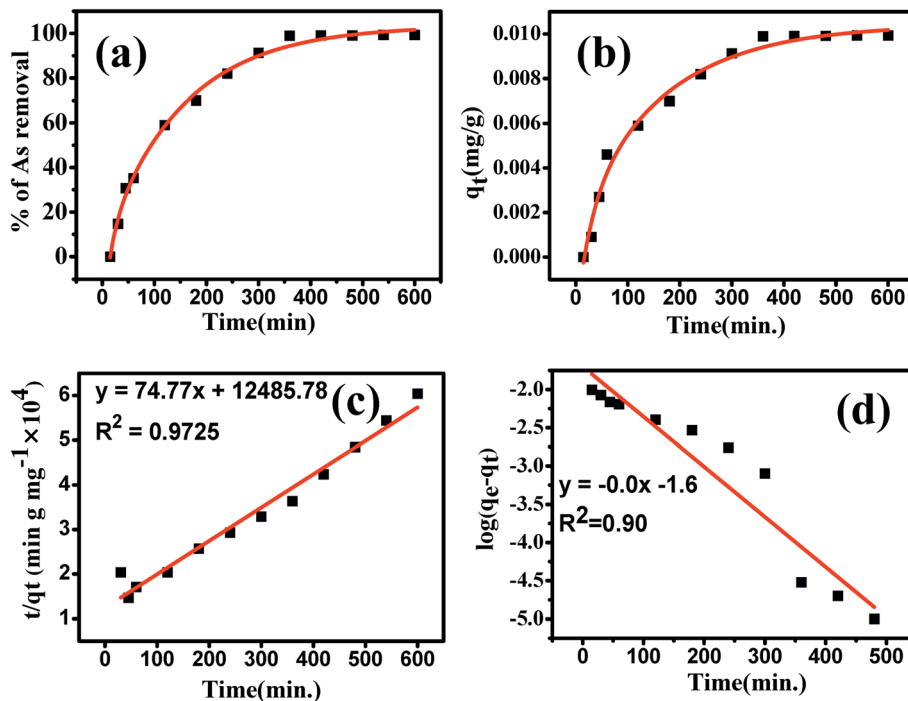
Fig. 7 Effect of time on (a) As(v) removal, (b) adsorption capacity (q_t) of As(v), (c) pseudo second order kinetics and (d) pseudo first order kinetics.
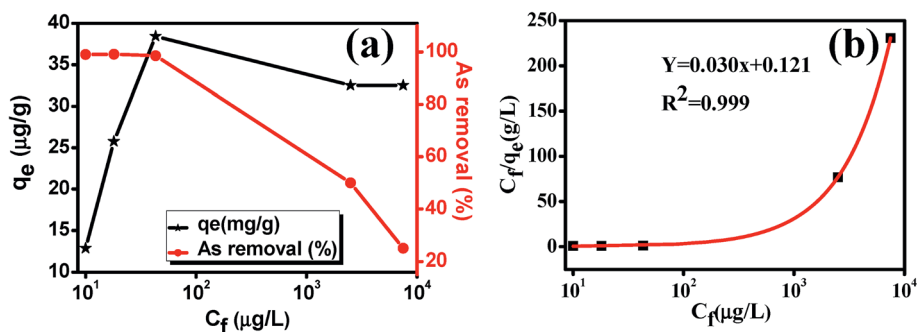

Fig. 8 (a) Effect of remaining concentration of As(v) on adsorption capacity of carbon foam, and (b) Langmuir adsorption isotherm.

where C_f (mg L^{-1}) is the remaining concentration of As(v), q_e (µg g^{-1}) is the adsorption capacity at equilibrium, q_m (µg g^{-1}) is the maximum adsorption capacity, K_L (L µg^{-1}) is the energy of reaction.

The value of K_L and q_m were calculated from linear plot of 'C_f/q_e' vs. 'C_f' as shown in Fig. 8(b). The value of K_L, q_m, and R^2 were found to be 0.248 L µg^{-1}, 38.44 µg g^{-1} and 0.999 respectively. The value of regression coefficient was found to be 0.999, which follows Langmuir isotherm. On the basis of Langmuir isotherm, it can be concluded that there is a monolayer adsorption over carbon foam surface. The value of separation factor (R_L) was calculated using eqn (10) as given below;

$$R_L = \frac{1}{1 + (K_L C_i)} \tag{10}$$

In the above equation, C_i denotes initial concentration of arsenic solution, K_L is Langmuir constant. The separation factor (R_L) value describes the nature of adsorption as given below;

$$R_L > 1 \text{ unfavourable,}$$

$$R_L = 0 \text{ then linear,}$$

$$0 < R_L < 1 \text{ favourable,}$$

$$R_L > 0 \text{ irreversible}$$

On the basis of above assumptions, separation factor,[47] the value of R_L was found less than 1, which suggest feasibility of the process and adsorption of As(v) over the surface of carbon foam is favourable.
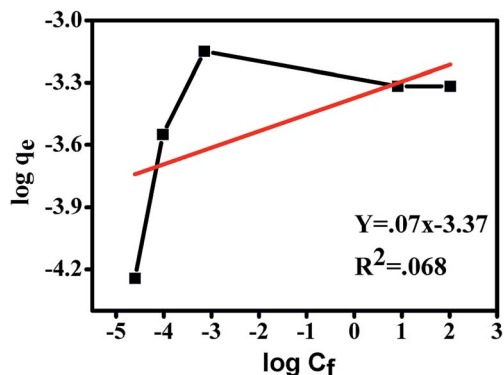
Fig. 9 Freundlich adsorption isotherm.

The Freundlich isotherm has also been studied to know the heterogeneous nature of carbon foam. The data has been fitted in Freundlich adsorption isotherm as given below

$$q_e = K_f C_f^{1/n} \qquad (11)$$

$$\log q_e = \log K_f + 1/n \log C_f \qquad (12)$$

where; 'K_f' and '$1/n$' are Freundlich parameters which represent distribution coefficient (L g^{-1}) and intensity of adsorption respectively. The regression coefficient value was obtained as 0.068 which is very less as a result the adsorption of arsenic is found homogeneous nature and does not follow Freundlich adsorption isotherm as show in Fig. 9.

3.5. Reusability of carbon foam

The reusability of carbon foam has been investigated after treating used carbon foam with 5% solution of EDTA and HNO$_3$ solution. First the used carbon foam was sonicated in 5% solution of EDTA and HNO$_3$ separately for one hour.

The decanted solutions were checked for leached concentration of As(v) by AAS-HG. It has been found that most of As(v) releases from the carbon foam surface. The same observations were further confirmed by SEM-EDX analysis as given in Fig. 10(a–d). The EDTA is a strong chelating agent and makes complexes with As(v). In the same way As(v) probably forms arsenic acid after treating with HNO$_3$ solution as given in chemical eqn (13).
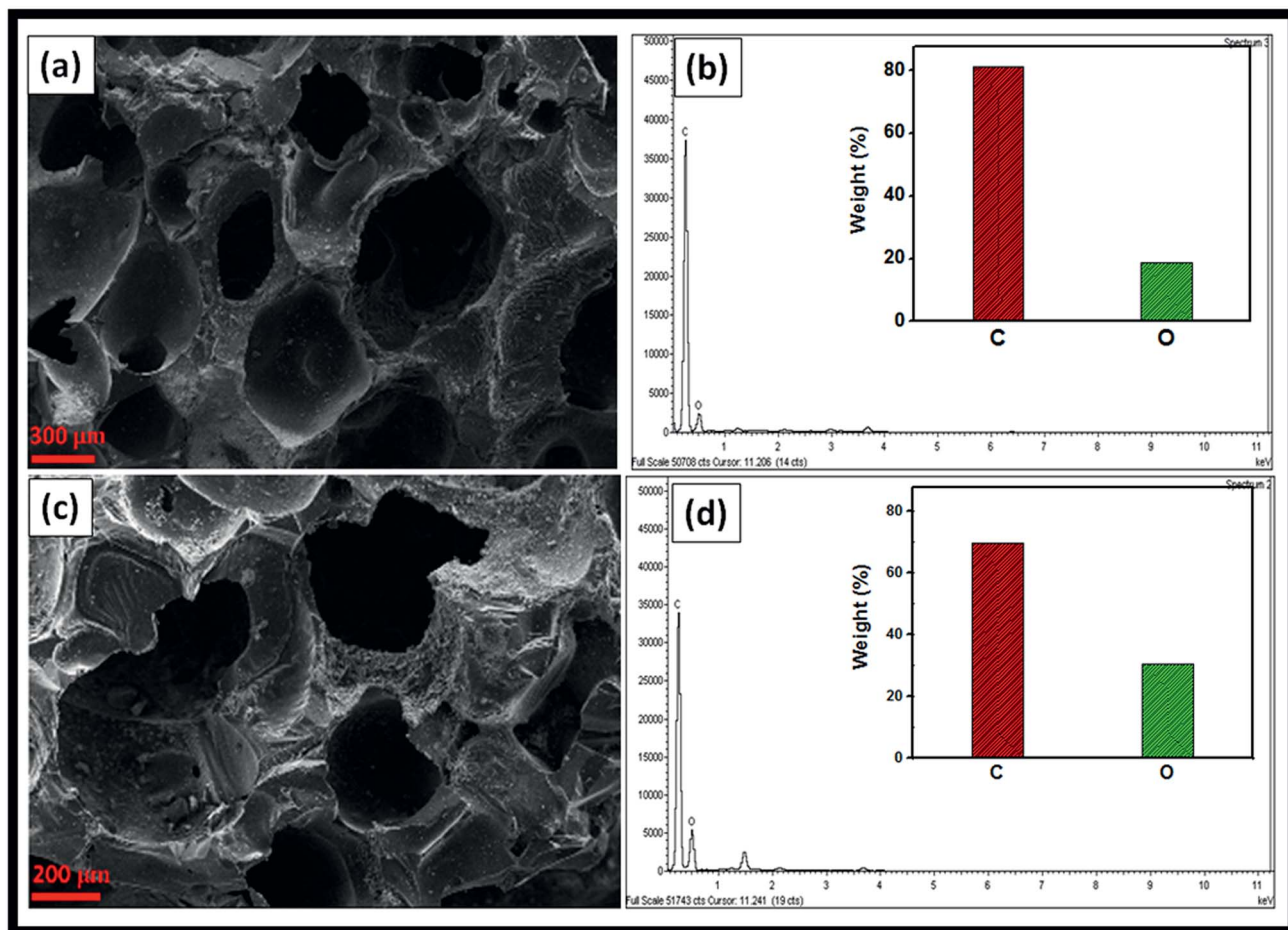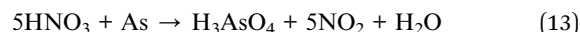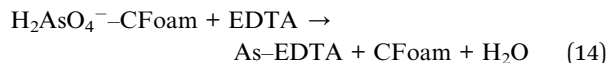
$$5HNO_3 + As \rightarrow H_3AsO_4 + 5NO_2 + H_2O \qquad (13)$$

Fig. 10 SEM and EDX of used carbon foam (a) and (b) after treated with EDTA, (c) and (d) after treated with HNO$_3$.

$$H_2AsO_4^- - CFoam + EDTA \rightarrow$$
$$As-EDTA + CFoam + H_2O \quad (14)$$

Furthermore, the EDX data of carbon foam shows that when the carbon foam is treated by HNO_3, the oxygen content is increased to 30.4% as compare to carbon foam treated by EDTA, the increase in oxygen content is due the oxidation of carbon foam by HNO_3 since HNO_3 act as strong oxidising agent. Further, after removal of As(v), the carbon foam was treated with HNO_3 and thoroughly washed with de-ionised water followed by drying at 105 °C, the same material was used in second cycle at optimized condition. In the second cycle, 83.2% of arsenic gets adsorbed. In the same way the carbon foam was used after treated with HNO_3 for third, fourth and fifth cycle having arsenic adsorption 60.1, 37.5 and 23.2% respectively. Furthermore, as carbon foam treated with HNO_3 up to five times, the % of arsenic removal decreased this is due to the decreasing of active sites on the surface of carbon foam.

4. Conclusions

In the present study, we report a cost effective method to synthesize novel 3D lightweight carbon foam from phenolic resin using PU template method. The SEM-EDAX, FTIR, XRD and XPS results indicating the adsorption of As(v) over the surface of carbon foam. The arsenic accumulated on the surface of carbon foam and water was purified upto safe potability limits of WHO and USEPA. The adsorption process followed Langmuir isotherm model suggesting monolayer adsorption. At optimized condition the maximum adsorption capacity of carbon foam for As(v) was found to be 38.4 $\mu g\ g^{-1}$ in the pH range 4–5. Moreover carbon foam is nontoxic, easy to fabricate, affordable and insoluble in water. Raw material for fabrication of carbon foam is easily available everywhere. There is no requirement of any costly equipment for fabrication of carbon foam and filtration unit to separate carbon foam from water after adsorption process. Such material can be safely used in remote areas where there is scarcity of power supply. Therefore, from the practical point of view, the proposed carbon foam should be promising adsorbent for the removal of As(v) from drinking water.

Acknowledgements

References

1 Y. Zhang, M. Yang and X. Huang, *Chemosphere*, 2003, **51**, 945–952.

2 L. Keith and W. Telliard, *Environ. Sci. Technol.*, 1979, **13**, 416–423.

3 S. V. Mohan, P. Nithila and S. J. Reddy, *J. Environ. Sci. Health, Part A: Environ. Sci. Eng. Toxic Hazard. Subst. Control*, 1996, **31**, 283–289.

4 E. Levy, *US Pat.*, 5,133,871, 1992.

5 R. Stone, *Science*, 2008, **321**, 184–185.

6 Y.-L. Ren, H.-Y. Wu, M.-M. Lu, Y.-J. Chen, C.-L. Zhu, P. Gao, M.-S. Cao, C.-Y. Li and Q.-Y. Ouyang, *ACS Appl. Mater. Interfaces*, 2012, **4**, 6436–6442.

7 T. Wang, L. Zhang, H. Wang, W. Yang, Y. Fu, W. Zhou, W. Yu, K. Xiang, Z. Su and S. Dai, *ACS Appl. Mater. Interfaces*, 2013, **5**, 12449–12459.

8 S. Yamamura, J. Bartram, M. Csanady, H. G. Gorchev and A. Redekopp, *Arsenic, Water, and Health: The State of the Art*, ed. H. Hashizume and S. Yamamura, World Health Organisation, 2003.

9 I. Ali, V. K. Gupta, T. A. Khan and M. Asim, *Int. J. Electrochem. Sci.*, 2012, **7**, 1898–1907.

10 K. A. Graeme and C. V. Pollack, *The Journal of emergency medicine*, 1998, **16**, 171–177.

11 E. Fogarassy, I. Galambos, E. Bekassy-Molnar and G. Vatai, *Desalination*, 2009, **240**, 270–273.

12 N. Balasubramanian, T. Kojima, C. A. Basha and C. Srinivasakannan, *J. Hazard. Mater.*, 2009, **167**, 966–969.

13 K. Vaaramaa and J. Lehto, *Desalination*, 2003, **155**, 157–170.

14 B. V. Tangahu, S. R. Sheikh Abdullah, H. Basri, M. Idris, N. Anuar and M. Mukhlisin, *Int. J. Chem. Eng.*, 2011, **2011**, 31.

15 K. Mozafarian, S. S. Madaeni and M. Khoshnodie, *Water Wastewater*, 2007, **17**, 22–28.

16 V. Chandra, J. Park, Y. Chun, J. W. Lee, I.-C. Hwang and K. S. Kim, *ACS Nano*, 2010, **4**, 3979–3986.

17 D. Mohan and C. U. Pittman, *J. Hazard. Mater.*, 2007, **142**, 1–53.

18 M. Elizalde-González, J. Mattusch, W.-D. Einicke and R. Wennrich, *Chem. Eng. J.*, 2001, **81**, 187–195.

19 Z. Liu, F.-S. Zhang and R. Sasai, *Chem. Eng. J.*, 2010, **160**, 57–62.

20 O. Thirunavukkarasu, T. Viraraghavan and K. Subramanian, *Water, Air, Soil Pollut.*, 2003, **142**, 95–111.

21 J. A. Wilkie and J. G. Hering, *Colloids Surf., A*, 1996, **107**, 97–110.

22 W. Zhang, P. Singh, E. Paling and S. Delides, *Miner. Eng.*, 2004, **17**, 517–524.

23 G. T. Schmidt, N. Vlasova, D. Zuzaan, M. Kersten and B. Daus, *J. Colloid Interface Sci.*, 2008, **317**, 228–234.

24 F. Di Natale, A. Erto, A. Lancia and D. Musmarra, *Water Res.*, 2008, **42**, 2007–2016.

25 A. K. Gupta, D. Deva, A. Sharma and N. Verma, *Ind. Eng. Chem. Res.*, 2010, **49**, 7074–7084.

26 V. K. Upadhyayula, S. Deng, M. C. Mitchell and G. B. Smith, *Sci. Total Environ.*, 2009, **408**, 1–13.

27 K. Lü, G. Zhao and X. Wang, *Chin. Sci. Bull.*, 2012, **57**, 1223–1234.

28 H. Liu, K. Zuo and C. D. Vecitis, *Environ. Sci. Technol.*, 2014, **48**, 13871–13879.

29 S. Vadahanambi, S.-H. Lee, W.-J. Kim and I.-K. Oh, *Environ. Sci. Technol.*, 2013, **47**, 10510–10517.

30 S Addo Ntim and S. Mitra, *J. Chem. Eng. Data*, 2011, **56**, 2077–2083.

31 N. Mahanta and J. P. Chen, *J. Mater. Chem. A*, 2013, **1**, 8636–8644.

32 X. Chen, K. F. Lam, Q. Zhang, B. Pan, M. Arruebo and K. L. Yeung, *J. Phys. Chem. C*, 2009, **113**, 9804–9813.

33 Z. Wu and D. Zhao, *Chem. Commun.*, 2011, **47**, 3332–3338.

34 D. M. Burke, M. A. Morris and J. D. Holmes, *Sep. Purif. Technol.*, 2013, **104**, 150–159.

35 C.-G. Lee, J.-W. Jeon, M.-J. Hwang, K.-H. Ahn, C. Park, J.-W. Choi and S.-H. Lee, *Chemosphere*, 2015, **130**, 59–65.

36 A. Yadav, R. Kumar, G. Bhatia and G. Verma, *Carbon*, 2011, **49**, 3622–3630.

37 R. Kumar, A. P. Singh, M. Chand, R. P. Pant, R. K. Kotnala, S. K. Dhawan, R. B. Mathur and S. R. Dhakate, *RSC Adv.*, 2014, **4**, 23476–23484.

38 R. Kumar, S. R. Dhakate, T. Gupta, P. Saini, B. P. Singh and R. B. Mathur, *J. Mater. Chem. A*, 2013, **1**, 5727–5735.

39 S. R. Dhakate, R. Kumar, R. B. Mathur and P. Saini, *US Pat.*, 20,150,305,211, 2015.

40 N. Fiol and I. Villaescusa, *Environ. Chem. Lett.*, 2009, **7**, 79–84.

41 N. Singh, A. Sarkar, R. Ramchandran and K. Lal, *Asian J. Chem.*, 2003, **15**, 1327–1330.

42 S. Zhang, X.-y. Li and J. P. Chen, *Carbon*, 2010, **48**, 60–67.

43 S. Zhang, X.-y. Li and J. P. Chen, *J. Colloid Interface Sci.*, 2010, **343**, 232–238.

44 K. Wu, R. Liu, T. Li, H. Liu, J. Peng and J. Qu, *Chem. Eng. J.*, 2013, **226**, 393–401.

45 C. Karthika and M. Sekar, *Res. J. Environ. Sci.*, 2012, **1**, 34–41.

46 I. Langmuir, *J. Am. Chem. Soc.*, 1918, **40**, 1361–1403.

47 K. R. Hall, L. C. Eagleton, A. Acrivos and T. Vermeulen, *Ind. Eng. Chem. Fundam.*, 1966, **5**, 212–223.